Am J Physiol Heart Circ Physiol 317: H1125–H1133, 2019.
First published September 20, 2019; doi:10.1152/ajpheart.00193.2019.

RESEARCH ARTICLE | *Integrative Cardiovascular Physiology and Pathophysiology*

On the importance of the nonuniform aortic stiffening in the hemodynamics of physiological aging

Stamatia Z. Pagoulatou,[1] Vasiliki Bikia,[1] Bram Trachet,[1,2] Theodore G. Papaioannou,[3] Athanase D. Protogerou,[4] and Nikolaos Stergiopulos[1]

[1]*Laboratory of Hemodynamics and Cardiovascular Technology, Institute of Bioengineering, Ecole Polytechnique Fédérale de Lausanne, Lausanne, Switzerland;* [2]*Institute of Biomedical Technology, IBiTech-bioMMeda, Ghent University, Ghent, Belgium;* [3]*Biomedical Engineering Unit, First Department of Cardiology, Medical School, National and Kapodistrian University of Athens, Athens, Greece; and* [4]*Cardiovascular Prevention and Research Unit, Department of Pathophysiology, National and Kapodistrian University Athens School of Medicine, Athens, Greece*

Submitted 25 March 2019; accepted in final form 9 September 2019

Pagoulatou SZ, Bikia V, Trachet B, Papaioannou TG, Protogerou AD, Stergiopulos N. On the importance of the nonuniform aortic stiffening in the hemodynamics of physiological aging. *Am J Physiol Heart Circ Physiol* 317: H1125–H1133, 2019. First published September 20, 2019; doi:10.1152/ajpheart.00193.2019.—Mathematical models of the arterial tree constitute a valuable tool to investigate the hemodynamics of aging and pathology. Rendering such models as patient specific could allow for the assessment of central hemodynamic variables of clinical interest. However, this task is challenging, particularly with respect to the tuning of the local area compliance that varies significantly along the arterial tree. Accordingly, in this study, we demonstrate the importance of taking into account the differential effects of aging on the stiffness of central and peripheral arteries when simulating a person's hemodynamic profile. More specifically, we propose a simple method for effectively adapting the properties of a generic one-dimensional model of the arterial tree based on the subject's age and noninvasive measurements of aortic flow and brachial pressure. A key element for the success of the method is the implementation of different mechanisms of arterial stiffening for young and old individuals. The designed methodology was tested and validated against in vivo data from a population of $n = 20$ adults. Carotid-to-femoral pulse wave velocity was accurately predicted by the model (mean error = 0.14 m/s, SD = 0.77 m/s), with the greatest deviations being observed for older subjects. In regard to aortic pressure, model-derived systolic blood pressure and augmentation index were both in good agreement (mean difference of 2.3 mmHg and 4.25%, respectively) with the predictions of a widely used commercial device (Mobil-O-Graph). These preliminary results encourage us to further validate the method in larger samples and consider its potential as a noninvasive tool for hemodynamic monitoring.

NEW & NOTEWORTHY We propose a technique for adapting the parameters of a validated one-dimensional model of the arterial tree using noninvasive measurements of aortic flow and brachial pressure. Emphasis is given on the adjustment of the arterial tree distensibility, which incorporates the nonuniform effects of aging on central and peripheral vessel elasticity. Our method could find application in the derivation of important hemodynamic indices, paving the way for novel diagnostic tools.

Address for reprint requests and other correspondence: S. Pagoulatou, Ecole Polytechnique Fédérale de Lausanne, STI IBI-STI Laboratory of Hemodynamics and Cardiovascular Technology, MED 3 2922 (Batiment MED), Station 9, CH-1015 Lausanne, Switzerland (e-mail: stamatia.pagoulatou@epfl.ch).

1-D simulations; hemodynamic monitoring; noninvasive

INTRODUCTION

Central hemodynamic parameters, such as aortic blood pressure and cardiac output, may have a greater prognostic value for assessing cardiovascular risk than peripheral hemodynamic indices (21). Although central hemodynamics are crucial for accurate diagnosis and optimal treatment management, there is an inherent difficulty in their noninvasive estimation in clinical practice. Most relevant central hemodynamic monitoring techniques proposed in the literature often involve statistical correlations (24), generalized transfer functions (3, 13), or formulas based on pulse wave analysis (9, 44).

The personalization of mathematical models of the cardiovascular system constitutes a physiologically relevant way for the derivation of central hemodynamic variables, a desirable alternative to most of the aforementioned techniques or commercial devices that lack a physiological/mathematical background. Particularly, patient-specific one-dimensional (1-D) simulations could serve as a valuable tool for the assessment of pressure and flow in the entire arterial network, which is crucial to disease initiation and progression (20). This is, of course, a challenging task, primarily because of the large amount of input data needed for the effective personalization of a distributed arterial tree model.

In a previous publication, we proposed a methodology for tuning the parameters of a validated, generalized 1-D model of the arterial tree and the subsequent derivation of the cardiac contractility based on noninvasive measurements of brachial pressure and aortic flow (27). Using the measured aortic flow as the model input, we achieved the parameter tuning by essentially altering the compliance of all arterial vessels in a uniform way until the model predicted brachial pressure accurately. The assumption of a uniform scaling of the arterial compliance between different individuals and different physiopathological situations (e.g., aging, disease, etc.) is oversimplifying. Indeed, stiffening can take place locally or affect heterogeneously the local elastic properties of the arterial tree, and hence, the assumption of uniform global stiffening may compromise the accuracy of the model predictions.

On this note, a number of studies have published findings supporting the preferential stiffening of the central arteries with increasing age (14). In young adults, the distensibility gradient from proximal aorta to peripheral arteries is steep, with proximal aorta being very compliant [local pulse wave velocity (PWV) typically less than 4 m/s] and the peripheral muscular arteries significantly stiffer. Arterial stiffening with age takes place in a nonuniform way, with stiffening being much more pronounced in the proximal aorta than in the peripheral arteries (14). In a previous work, we studied the implications of this age-related nonuniform stiffening on the wave transmission characteristics and reported a significant increase in the forward wave amplitude with age as well as a decrease in pulse pressure amplification from central to peripheral arteries (26).

In consideration of the aforementioned facts, the present work aimed at highlighting the importance of considering the age-related nonuniform stiffening of the arteries when adapting the parameters of the arterial tree. Concretely, we developed a methodology that uses as model inputs the subject's age, aortic flow, and peripheral blood pressure and accordingly adjusts the arterial parameters. More particularly, the compliance of the central and peripheral arterial segments is adjusted differently for younger and older individuals according to literature trends on the evolution of the aortic stiffness with aging. The proposed methodology was tested and validated against in vivo data from a population of both healthy and diseased adults. We find that the tuned arterial tree models are capable of accurately capturing the elastic properties of the aorta and the hemodynamic profile of each subject, reproducing the expected pressure phenotypes. Finally, these tools could possibly be further exploited to derive central hemodynamic indices of importance, such as central pressures.

MATERIALS AND METHODS

Brief description of the 1-D model of the arterial tree. The generic 1-D model of the systemic circulation, previously developed (38) and validated (37) by Reymond et al., consists of 103 arterial segments (Fig. 1) that are considered as flexible tapered tubes. The governing equations are based on the integration of the continuity and momentum conservation equations over the arterial cross section complemented with a constitutive relation relating distending pressure and cross-sectional area. The wall shear stress is approximated using the Witzig-Womersley theory (52). The arterial wall behavior is viscoelastic and nonlinearly elastic (11), whereby the local arterial compliance has a pressure-dependent component (C_p) and a location-dependent component (C_d) (15). The latter function can be calculated for a reference pressure of $P_{ref} = 100$ mmHg and for an average cross-sectional area (A) according to the local pulse wave velocity:

$$C_d(d) = \frac{A}{\rho \mathrm{PWV}^2(d)}$$

In the initial 1-D model of Reymond et al. (38), a global empirical relationship relating PWV and vessel diameter was developed based on previously published data for a healthy young male adult. At the terminal sites, the vascular beds are modeled using 3-element Windkessel models, in which the distribution of terminal resistance in proximal and distal resistances was chosen so that it yields minimal reflections. At the proximal end, the arterial tree either receives a prescribed aortic flow waveform or is coupled with a time-varying elastance model of the left ventricle (40, 42).

Considerations on nonuniform arterial stiffening along the aorta. The arterial compliance and especially its location-dependent component $C_d(d)$ vary significantly between individuals. Compliance is affected by many factors, with age being the predominant one. A study by Cho et al. (4) compared young and old patients with untreated hypertension and showed that the young hypertensive group

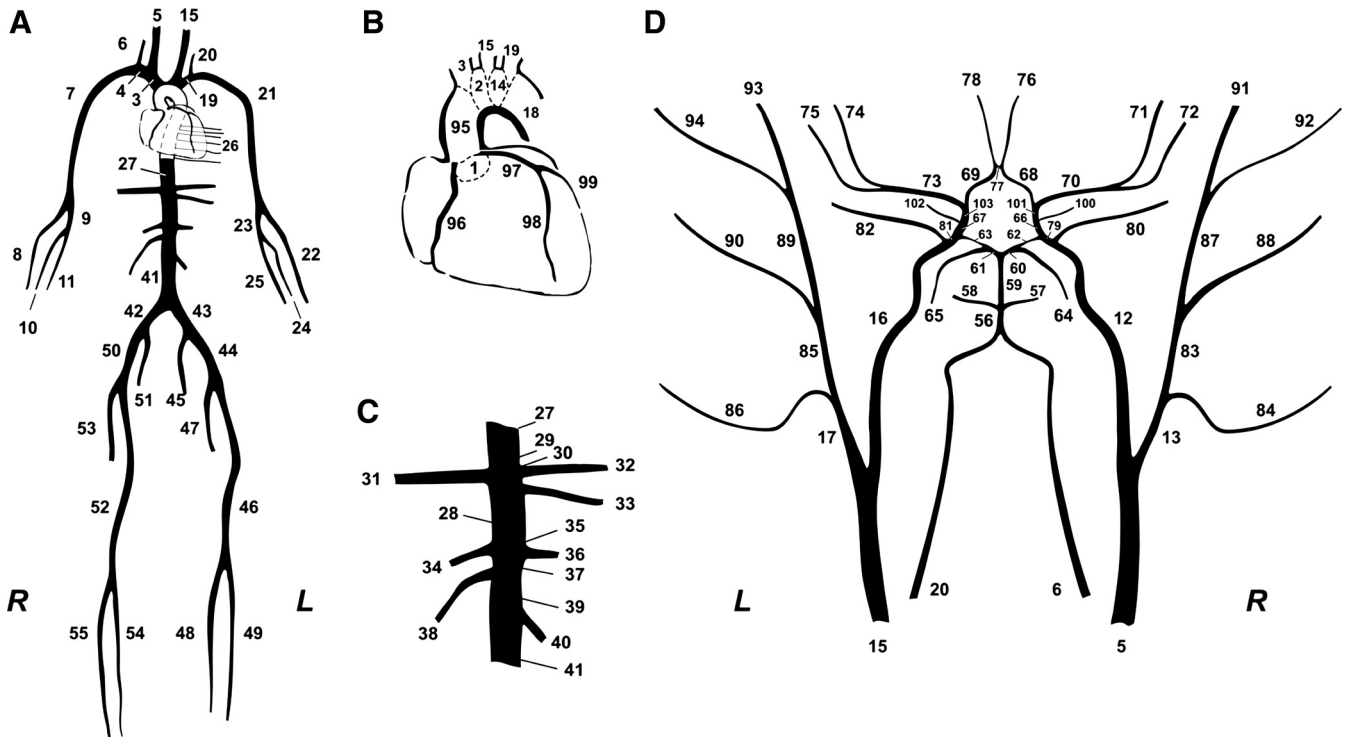

Fig. 1. Schematic representation of the arterial tree developed by Reymond et al. (38) consisting of 55 main arteries of the systemic circulation (*A*), the circulation in the coronaries (*B*), the principal abdominal aortic branches (*C*), and the circle of Willis (*D*). Adapted from Reymond et al. (38). Used with permission.

had significantly lower central PWVs than the older age group, despite showing higher levels of peripheral blood pressure. This suggests that PWV is mainly affected by age rather than blood pressure levels.

In terms of model personalization, the local PWV should ideally be known for all arterial locations to precisely calculate the compliance of a patient's arterial tree. Of particular interest is the compliance gradient along the aorta, which is substantially altered during aging. Aging leads to gradual and nonuniform loss of the elasticity of the arteries, whereby the central aorta is more affected than the periphery (14). As a result of this heterogeneous alteration, the pressure waveforms in older subjects, often referred to as *Type A* waveforms, are characterized by a dominant late systolic peak and a shoulder with inflection on the upstroke (22). The dominant late systolic peak is primarily attributed to augmented forward wave component amplitude because of the stiffened proximal aorta and, to a lesser extent, to augmented and earlier arriving reflections (22, 26). In previous work, we incorporated this nonuniform stiffening of the arterial tree with age into the model by developing averaged distensibility curves for each age decade from 30 to 80 yr based on literature data and were able to reproduce the expected aortic pressure wave shapes (26).

To show the importance of nonuniform aortic stiffening in the development of aortic systolic hypertension while preserving the "correct" aortic phenotype, Reymond et al. (39) simulated aortic stiffening with age in two ways: first, by equally reducing compliance uniformly in all arteries ("global stiffening"), and second, by applying a nonuniform stiffening, whereby, in accordance to observations, proximal aorta is stiffened more than peripheral vessels ("local stiffening"). The results are shown in Fig. 2. The reduction in total arterial compliance was the same (−29%) in both global and local stiffening. Both global and local stiffening yielded the same pulse pressure increase of 45% and the same systolic pressure in the root of the proximal aorta; however, local nonuniform stiffening was the one that produced a physiologically relevant aortic pressure phenotype, more closely resembling the *Type A* waveforms. Reymond et al. (39) also noted that a decrease in compliance under local proximal aortic stiffening leads to higher carotid-to-femoral pulse wave velocities (c-f PWV) when compared with global stiffening, the difference being attributed to the more pronounced stiffening of the aortofemoral path.

Method for adaptation of the distensibility-diameter curve. Based on the aforementioned observations, we put forward the following methodology for incorporating the effects of aging during the adaptation of the 1-D arterial model. For young subjects, we simply apply global stiffening of the arterial tree, meaning that the area compliances of all arteries are scaled with one global scaling factor. For older individuals, we apply the local stiffening approach, whereby compliance of only the aortic segments (segments 1-95-2-14-18-27 of the arterial tree, as shown in Fig. 1) is adjusted. In detail, the subject is initially categorized according to his/her age in the younger or older age group. The age of 50 yr was used as the cutoff value for grouping in the present study, as vascular aging is reported to accelerate after this threshold (4). As an initial approximation of the subject's arterial tree, we use the "average" arterial compliance values expected for his/her age, as presented in our previous aging model (26). The simulation runs using the recorded aortic flow as model input. Subsequently, we compare the model-predicted brachial systolic blood pressure (SBP) and diastolic blood pressure (DBP) to the measured values, and if the error is significant, we adjust the arterial compliance applying either global or local stiffening. Peripheral resistance is also calculated and adjusted as the ratio of the mean arterial pressure over the measured cardiac output. Finally, the arterial geometry is adjusted according to the measured aortic diameter via multiplication of all internal diameters with a uniform factor.

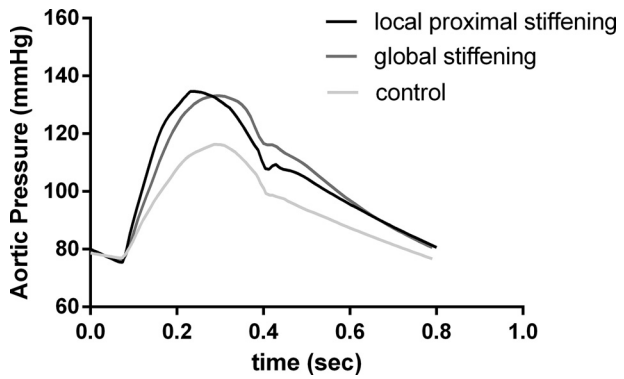

Fig. 2. Pressure waveforms at the proximal ascending aorta for the control case (light gray line), after local proximal stiffening (black line) and global arterial stiffening (gray line) for the same pulse pressure increase (+45%).

Validation against in vivo data. The method described above was tested with in vivo data collected previously by Papaioannou et al. (31). Method accuracy and bias were assessed by comparing *1*) the model-estimated carotid-to-femoral PWV with the corresponding values measured by a reference technique (SphygmoCor, AtCor, Sydney, Australia) and *2*) the model-estimated aortic pressure (in terms of both magnitude and shape) with the predictions from the Mobil-O-Graph device (IEM, Stolberg, Germany).

The database included the hemodynamic and cardiovascular recordings from 24 patients who underwent noninvasive cardiovascular risk assessment. Out of the 24 patients, 4 were excluded from the study, as their cardiac ultrasound or applanation tonometry data were lacking or unreliable for use. The study population included both sexes and covered a variety of health conditions, including hypertension, cardiovascular disease, and stroke (31).

Data recording and analysis. During the in vivo investigation, two repeated measurements of the proximal aortic peak velocity profile were acquired via transthoracic two-dimensional Doppler echocardiography. Both measurements were conducted by an experienced cardiologist at supine position and according to the recommendations of Quiñones et al. (34). Blood flow was calculated from the peak velocity profiles following the Witzig–Womersley theory (52) and assuming a constant cross-sectional area. The model input aortic flow was set equal to the average of the two measured flow curves.

Peripheral systolic and diastolic pressure values were recorded at the brachial artery using the Mobil-O-Graph device, which has been thoroughly validated in the past (50). This device also allows for the reconstruction of the aortic pressure and the extraction of key waveform features, such as the central augmentation index (AIx). The central AIx is a measure of wave reflections and reflects the percentage of the total pulse pressure that can be attributed to the reflected pulse wave (22). A number of studies have previously validated the use of the Mobil-O-Graph for noninvasive estimation of central pressure (18, 33, 49, 51). Accordingly, good agreement has been shown between Mobil-O-Graph-derived AIx and those from other common tonometric devices (47). In our study, both estimates of aortic SBP and AIx were extracted and were thereafter used as reference values.

Carotid-to-femoral PWV was measured via applanation tonometry using the SphygmoCor system, which has the advantage of recording signals of carotid and femoral pressure in parallel, thus avoiding the need of synchronization. This device is also often used for the reconstruction of the aortic pressure wave (13) from the recorded radial pressure waves (30) and has shown quite reliable results in previous validation studies (28, 32). However, in the present study, we used the Mobil-O-Graph data as reference for the aortic pressure to ensure that the recordings of peripheral pressure and the estimates of central pressure were simultaneous, as discussed below. More details on the measurement protocol can be found in the original publication (31).

For each patient, we used the recorded data and the methodology described above to tune the arterial tree parameters proximally and distally. The tuned models allowed for the derivation of the c-f PWV, which was calculated analytically by the compliance of each arterial

Table 1. *Hemodynamic values of the study population categorized into the two age groups*

	Total Sample	Age Group I (Age < 50 yr)	Age Group II (Age ≥ 50 yr)	*P* Value
n	20	16	4	
Men/Women, *n*	11/9	8/8	3/1	0.59
Age, yr	38.4 ± 13.6	32.3 ± 5.1	62.5 ± 7.9	<0.05
Central SBP, mmHg	110.0 ± 11.2	108.9 ± 11.6	114.4 ± 9.2	0.33
Central DBP, mmHg	78.6 ± 8.8	77.3 ± 8.4	83.6 ± 10.0	0.26
Peripheral SBP, mmHg	116.3 ± 10.7	115.0 ± 11.1	121.5 ± 8.2	0.24
Peripheral DBP, mmHg	77.6 ± 8.7	76.4 ± 8.2	82.4 ± 10.1	0.35
c-f PWV, m/s	6.9 ± 1.9	6.0 ± 0.6	10.3 ± 0.9	<0.05
HR, beats/min	70.4 ± 10.3	69.7 ± 10.6	73.0 ± 10.1	0.70
CO, L/min	4.2 ± 1.0	4.0 ± 0.9	5.1 ± 1.1	0.07

c-f PWV, carotid-to-femoral pulse wave velocity; CO, cardiac output; DBP, diastolic blood pressure; HR: heart rate; SBP, systolic blood pressure.

segment in the aortic-femoral path based on the Bramwell-Hill equation. Furthermore, the model-produced proximal aortic pressure curves were processed to derive the SBP and the central AIx, as explained in Murgo et al. (22). The computed values were then compared with the corresponding estimates of the Mobil-O-Graph device.

Statistical analysis. Correlation, accuracy, and agreement between the model-based estimates and the in vivo recordings of c-f PWV were assessed using the Pearson's (r) and Spearman's (ρ) correlation coefficients, the intraclass correlation coefficient, the normalized root mean square error (nRMSE), and the Bland–Altman analysis (1). High values of r and ρ reflect good correlation in terms of linearity and direction. Bias was estimated by the mean difference ($\bar{d}$) and the standard deviation of the differences (SD). The limits of agreement were set at $\bar{d}$ + 2SD and $\bar{d}$ − 2SD, as 95% of the prediction errors for a normal distribution are expected to lie in this range. The Bland–Altman analysis was further used to assess the agreement between the model-derived aortic pressure and AIx with the respective estimates of the Mobil-O-Graph. The Mann–Whitney nonparametric test was used for the evaluation of differences of continuous variables between the two age groups. Statistical significance was accepted for P values <0.05. Data analysis was performed using the GraphPad Prism software and Matlab.

RESULTS

Table 1 summarizes the hemodynamic parameters of the 20 patients, separated into 2 age groups (below and above 50 yr old). Cardiac output, central and peripheral blood pressure, and c-f PWV are reported. As expected, the younger age group (n = 16) exhibited significantly lower carotid-to-femoral pulse wave velocities than the older group (n = 4).

Figure 3*A* shows a box plot of the model estimates against the measured c-f PWV values along with their confidence intervals. The Bland–Altman plot in Fig. 3*B* depicts the difference between the model-derived c-f PWV values and the respective SphygmoCor c-f PWV values against their mean. The limits of agreement are also illustrated by the two horizontal continuous lines. The mean error in the estimation of c-f PWV was 0.14 m/s, with limits of agreement equal to 1.7 and −1.4 m/s. The greatest deviations are observed at high c-f PWVs; it should be noted, however, that for these c-f PWV values, the confidence intervals of the reference device were wide, in the order of magnitude of 1 m/s. An overview of statistical parameters of agreement, accuracy, and correlation is also given in Table 2.

Table 2. *Indices of correlation, accuracy, and agreement between the measured and method-derived c-f PWV values*

Correlation	
Pearson's correlation coefficient, r	0.92
Spearman's correlation coefficient, ρ	0.99
Intraclass correlation coefficient	0.90
Accuracy	
Normalized root mean square error, %	11.1
Agreement	
Mean difference, $\bar{d}$, m/s	0.14
Standard deviation of difference, SD, m/s	0.77
Limits of agreement, m/s	1.68, −1.39

c-f PWV, carotid-to-femoral pulse wave velocity.

The scatterplots and Bland-Altman plots for the aortic systolic pressure and augmentation index as derived by the Mobil-O-Graph device and as predicted by the model are also shown in Fig. 4. The mean difference of aortic systolic pressure was equal to 2.3 mmHg, with SD of difference 3.0 mmHg. The nRMSE was 3.3%. It is noted that there is no particular trend of the differences to vary with the mean SBP. Accordingly, the model predictions for the AIx were in good agreement with the Mobil-O-Graph estimates; the mean difference was 4.25% with an SD of 3.7%.

Moreover, Fig. 5 depicts the aortic pressure waveforms as predicted by the tuned model for two different subjects. The left plot corresponds to the simulation results of a 52-yr-old man and the right plot to a 30-yr-old woman. We clearly observe that the pressure waveform for the older subject resembles the characteristic *Type A* phenotype, producing the anticipated shoulder with inflection at the upstroke. Conversely, for the younger subject, the model predicts a smooth upstroke, which resembles the *Type C* phenotype.

DISCUSSION

In this study, we presented a simple technique to tune the parameters of a previously validated 1-D model of the systemic

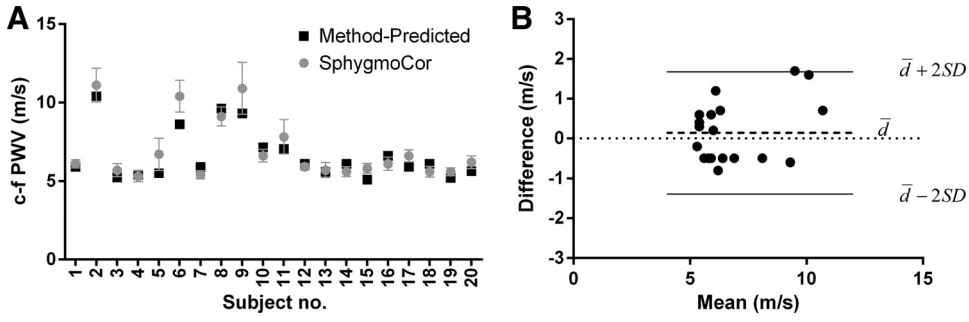

Fig. 3. *A*: Method-estimated carotid-to-femoral pulse wave velocity (c-f PWV) values plotted against the reference SphygmoCor values along with their respective confidence intervals. *B*: The Bland–Altman plot of the difference between the estimated and reference c-f PWV values against their means. Mean difference ($\bar{d}$) as well as 95% confidence intervals (±2SD around the mean difference) are depicted with continuous and dashed lines, respectively.

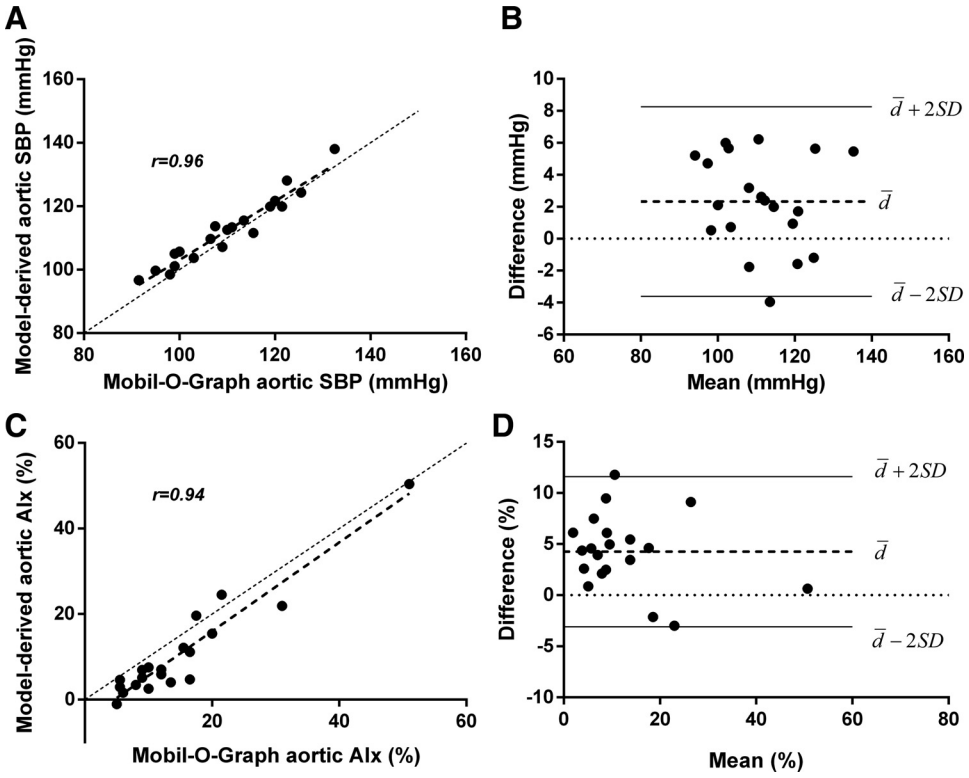

Fig. 4. *A*: Scatterplot of the aortic systolic blood pressure (SBP) as computed by the method and as predicted by the Mobil-O-Graph device. *B*: The Bland-Altman plot of the difference between the model-estimated and Mobil-O-Graph aortic SBP values against their means. *C* and *D*: The respective scatterplot and Bland-Altman plot for the central augmentation index as computed by the method and as predicted by the Mobil-O-Graph device. Mean difference ($\bar{d}$) as well as 95% confidence intervals (±2SD around the mean difference) are depicted with continuous and dashed lines, respectively. AIx, augmentation index.

circulation based on noninvasive measurements of proximal aortic flow and brachial sphygmomanometric pressure alone. This was motivated by *1*) our observations and experience from modeling the heterogeneous effects of aging on arterial distensibility and *2*) previous work from our group on the differential effects of different mechanisms of arterial stiffening on central hemodynamics (39). We hypothesized that it is possible to effectively tune the distensibility-diameter curve of the arterial tree by applying either a local proximal or global stiffness adjustment factor according to the patient's age.

The validation of the proposed arterial tree tuning methodology against in vivo data of both healthy and diseased adults yielded encouraging results. It was shown that the estimated carotid-to-femoral PWV, which is the most commonly used quantity as surrogate to aortic compliance, was in good agreement with the respective measurement of c-f PWV made by applanation tonometry (SphygmoCor apparatus). We reported a small bias, d = 0.14 m/s, and SD of differences, SD = 0.77 m/s. This small bias is quite lower than the observed intra-observed reproducibility of c-f PWV measurement (29). In general, the estimation errors were greater for the older subjects, whose c-f PWVs were higher. Although the older sample was small ($n = 4$), a limitation that is discussed more thoroughly below, we noted that the proposed technique was able to capture the expected pattern of increased c-f PWV for older ages. On the contrary, if we had employed only the global stiffening mechanism for the older adults, this would have led to a severe underestimation of the computed c-f PWVs; namely, it would have increased the average estimation error for the older group from −0.9 m/s to −3.7 m/s.

Interestingly, we found that, irrespective of the stiffening mechanism employed, the resulting increase in pulse pressure is dictated primarily by the loss in the total arterial compliance of the tree. In other words, the increase in pulse pressure seems not to be affected by the exact topology in which the stiffening occurs (nonuniform local or global) but rather by the overall compliance of the arterial tree. This finding is in good agreement with previous studies and supports the methodology by

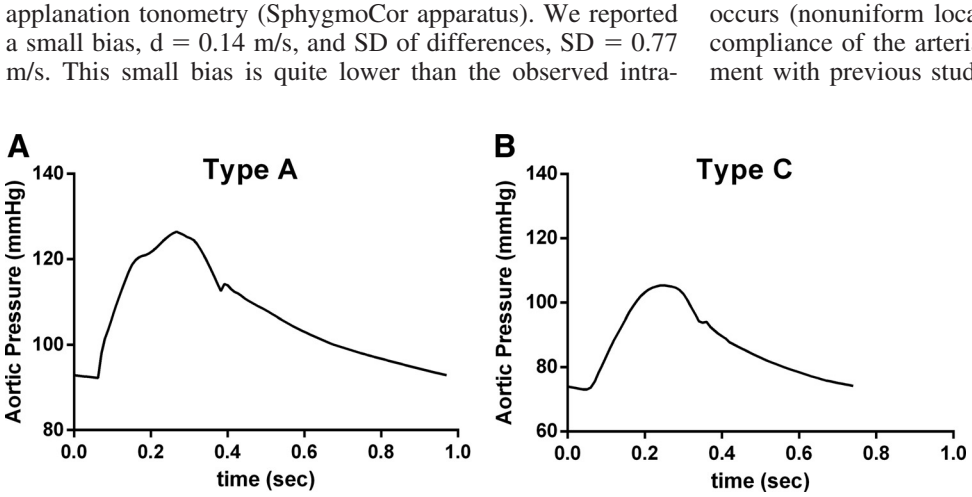

Fig. 5. Aortic pressure waveforms derived from the model simulations for 2 subjects: the characteristic *Type A* pressure phenotype of a 52-yr-old man (*A*) and the *Type C* phenotype of a 30-yr-old woman (*B*).

Stergiopulos et al. (41), who proposed the pulse pressure method, a simple two-element Windkessel-based method for the estimation of total arterial compliance.

It is important to note that the proposed technique might not achieve the exact personalization of the distributed model of the arterial tree, as it is based on an average model adjusted following population-averaged trends. However, as discussed before, the exact personalization of the arterial tree model presents major challenges, primarily because of the need of a large amount of input data. Conversely, our aim here was to highlight the importance of considering the nonuniform stiffening of the arterial tree when adjusting the model parameters for aged individuals. Accordingly, we developed "approximate" distributed models, which were capable of faithfully capturing key features of the hemodynamics of aging. In our simulations, we showed that we are able to replicate the characteristic aortic pressure phenotypes only by employing different stiffening mechanisms according to the subject's age (Fig. 5).

In that context, it is important to consider the possible application of these simulations to derive central indices noninvasively. For example, this technique could be combined with our previously proposed methodology (27) for the noninvasive estimation of the end-systolic elastance, an index that serves as the gold-standard measure of cardiac contractility and is therefore of particular interest to clinicians.

Another potential application of the presented method is the derivation of the central aortic pressure, which carries more valuable prognostic value for cardiovascular damage than peripheral pressure (46). Because of the importance of the central aortic pressure, a number of previous studies have proposed noninvasive methods for its derivation.

A recent study by Tosello et al. (43) developed and validated a technique for the estimation of central blood pressure via adjustment of a multiscale mathematical model according to brachial pressure, height, weight, age, left-ventricular end-systolic, and end-diastolic volumes and central PWV. The validation of their method showed significant overestimation of systolic blood pressure and underestimation of diastolic pressure when compared with the SphygmoCor device, with mean differences equal to 7.8 mmHg and −3.2 mmHg, respectively.

Another study (12) proposed a methodology for the adjustment of the distributed model parameters from measures of the proximal and distal radial pulse waves and the subsequent calculation of the aortic-to-radial transfer function. Their experimental results for central pressure estimation showed better performance than the broadly clinically used generalized transfer function and n-point moving average techniques.

A promising technique for deriving central blood pressure via a standard automatic arm cuff was proposed by Natarajan et al. (23). Their method leverages physiologic modeling to first accurately derive brachial blood pressure from the oscillogram and then calculates the central pressure via variable transfer functions, in which the pulse transit time is adjusted accordingly. Their technique was validated and found more reliable than other noninvasive devices.

Ghasemi et al. (10) recently published a paper on the estimation of cardiovascular risk from noninvasive pulse volume waveforms. Their method leverages the fact that pulse waves measured at peripheral sites, i.e., arm and ankle, both originate from the ascending aorta. Consequently, in a first step, they fit the parameters of a transmission line model according to multiple peripheral measurements. In a second step, they derive the central blood pressure waveform and then estimate cardiovascular risks. Their model was trained and validated with in vivo data from 164 subjects and showed better performance than the generalized transfer function. Ebrahimi Nejad et al. (8) also published a similar concept that relies on a model-parameter identification approach to assess cardiovascular risk. Their methodology employs a tube-load model of wave propagation and reflection, in which the proximal and distal blood pressure waveforms are inputted. The lumped parameter model is subsequently individualized, and the algorithm recognizes unphysiological patterns in the model parameters. Although this is a preliminary work and consists of a simplified model, it demonstrates the great potential of using vascular models for disease diagnosis.

The current method presents a significant advantage, as it employs a complete, distributed 1-D model of the arterial tree, in which the heterogeneous effects of aging on the arterial stiffness can be incorporated. In our study, we found that the estimated aortic systolic pressure was in good agreement with the estimates given by the Mobil-O-Graph device, the mean difference being 2.3 mmHg. We did not notice a particular trend for errors in the aortic SBP estimation as a function of age or hypertension. Accordingly, the method yielded accurate estimation of the aortic AIx. The central AIx is a hemodynamic parameter of importance, as it depends on the arterial stiffness and the reflective properties of the arteries (25). It is related to risk factors for cardiovascular disease and serves as predictor of morbidity and mortality (17, 45, 48). Therefore, there is potential in applying the proposed technique in the clinic as a noninvasive tool for central pressure monitoring and risk stratification. Our future work will investigate this potential by validating the method against invasive pressure data.

An interesting potential of the proposed modeling approach is that there can be an interchange between the model inputs and the output qualities. We showed that when age, aortic flow, and brachial pressure are known, it is possible to accurately estimate the compliance of the central arteries and thus effectively describe the arterial tree of a patient. This scheme could potentially be reformulated and adjusted to receive as inputs the age, central compliance, and brachial pressure of the patient and yield the cardiac output, the monitoring of which constitutes a major hurdle in actual clinical practice (16).

General considerations and limitations. An important point to be made pertains to the use of the carotid-to-femoral PWV as an accurate index of the aortic wall elasticity. Previous studies have questioned the utility of c-f PWV as a clinical measure of central stiffness and hence as a diagnostic marker for early vascular stiffening. More specifically, Cuomo et al. (5) undertook a fluid-structure interaction study to simulate the effects of aging on the regional wall properties of the human aorta and showed that c-f PWV correlated poorly with the circumferential stiffness (imposed on the model). Conversely, other metrics that are directly linked to arterial geometry, such as local distensibility, demonstrated better correlation with structural stiffness. These results were also corroborated by their subsequent study (6), which combined in vivo and in vitro data to build state-of-the-art, patient-specific fluid-structure interaction mouse models; they reported that changes in PWV did not effectively capture the regional differences in the

corresponding material stiffness properties, particularly when comparing between males and females. They suggested that this discrepancy can be attributed mainly to two factors, namely the dependency of PWV on the nonuniform arterial geometry (which is not accounted for in the simplified equation by Moens-Korteweg) and the use of an approximate path length between the 2 signal recordings [commonly assumed 80% of the direct tape-measured distance (36)].

Although these computational studies show poor correlation between c-f PWV and material properties, c-f PWV agrees well with regional measures of compliance. Previous studies, such as Boardman et al. (2), Dogui et al. (7), and Redheuil et al. (35), have shown that the c-f PWV is strongly related to measures of aortic arch compliance, but with a trend to overestimate it; conversely, it correlates better with descending and abdominal distensibility. This might be attributed to the fact that the carotid-to-femoral path excludes the ascending aorta and the aortic arch, which are highly compliant in the young.

In that context, we recognize that the c-f PWV is an average index of the aortic elasticity and might more reflect the properties of the descending thoracic and abdominal part. Therefore, in the present study, we can only maintain that the methodology effectively captures the average elastic properties of the aorta. Our future work will be oriented toward investigating the accuracy of the proposed method against detailed in vivo data on the regional PWV measured at multiple aortic sites.

As discussed above, despite having access to both the SphygmoCor and Mobil-O-Graph aortic pressure estimates, we chose to use only the latter values as a reference for our comparisons. This was done primarily to ensure that the reference aortic pressure was simultaneously recorded with the brachial pressure that drove the optimization process. Using the SphygmoCor reconstructed aortic pressure waves as reference values would significantly affect the accuracy of the estimation of aortic SBP reported; namely, the nRMSE would increase from 3.3% to 13.4%.

Furthermore, a few limitations of the present study need to be acknowledged. This method is based on a generalized model of the aging systemic circulation that was previously developed according to published data (26). As briefly discussed above, this entails that the tuned model does not necessarily represent the patient-specific conditions. It is rather an "approximately personalized" model, which, however, captures key hemodynamical indices. The tuning technique could be better refined to incorporate factors such as sex, body mass index, etc. Moreover, as the tuning algorithm was designed based on physiological data, the effects of certain pathologies (e.g., atherosclerosis, coronary artery disease, etc.) are not taken into account, and hence the quality of the tuning process and the resulting predictions may be compromised. Nevertheless, it should be noted that the in vivo validation of the method was conducted on a population of both physiological and pathological cases.

Methodological considerations regarding the measurement protocol have been presented in detail in the previous publication by Papaioannou et al. (31). As discussed above, the Mobil-O-Graph device does not provide a direct measurement of the aortic pressure but makes use of transfer functions to noninvasively estimate it. However, the use of this device is well justified given its good performance in previous validation studies. Although aging is related to an increase in SBP with a concomitant decrease in DBP (19), in our sample, the difference in SBP and DBP values between the two age groups was not found to be statistically significant. This can be attributed to the small sample size used as well as the fact that the study population included both healthy and diseased adults. The older age group includes only four subjects, limiting our ability to generalize our conclusions. Our database was extracted from a previous study that aimed at the validation of a novel method for cardiac output monitoring and thus did not focus on an equal distribution between young and old patients. Nevertheless, it is important to point out that this was essentially a proof-of-concept study. Despite the small sample size, our method was able to predict a significant difference in the estimated c-f PWV between the two age groups and produce the characteristic *Type A* pressure waveforms for the older subjects. This encourages us to continue the validation process in a greater sample of both sexes with different age groups and on a wider range of pathologic conditions.

In this study, we showed the importance of considering the heterogeneous effects of aging on the arterial distensibility when adapting the properties of a distributed model. We showed that if we differentiate between young and old subjects and accordingly employ different mechanisms of arterial stiffening, we are able to capture *1*) the expected increase in the carotid-to-femoral PWV with age and *2*) physiologically relevant aortic pressure waveforms, both in terms of magnitude (SBP) and wave reflections (AIx). Accordingly, we proposed a technique for effectively tuning a 1-D model of the arterial tree using noninvasive measurements and a previously developed model of the aging cardiovascular system. The proposed methodology was tested using in vivo data from a population of healthy and diseased subjects and showed encouraging results. The tuned models accurately predicted the carotid-to-femoral PWV and central systolic blood pressure, which encourages us to further investigate the method validity in larger samples. This in silico approach could find wide application in the derivation of central hemodynamic variables that are indispensable in the clinical reality, improving our understanding of central hemodynamics and paving the way for novel personalized diagnostic tools.

DISCLOSURES

No conflicts of interest, financial or otherwise, are declared by the authors.

AUTHOR CONTRIBUTIONS

S.Z.P. and N.S. conceived and designed research; S.Z.P., T.G.P., and A.D.P. performed experiments; S.Z.P. analyzed data; S.Z.P., V.B., and B.T. interpreted results of experiments; S.Z.P. prepared figures; S.Z.P. drafted manuscript; S.Z.P., V.B., B.T., T.G.P., A.D.P., and N.S. edited and revised manuscript; S.Z.P., V.B., B.T., T.G.P., A.D.P., and N.S. approved final version of manuscript.

REFERENCES

1. **Bland JM, Altman DG.** Statistical methods for assessing agreement between two methods of clinical measurement. *Lancet* 327: 307–310, 1986. doi:10.1016/S0140-6736(86)90837-8.
2. **Boardman H, Lewandowski AJ, Lazdam M, Kenworthy Y, Whitworth P, Zwager CL, Francis JM, Aye CY, Williamson W, Neubauer S, Leeson P.** Aortic stiffness and blood pressure variability in young people: a multimodality investigation of central and peripheral vasculature. *J Hypertens* 35: 513–522, 2017. doi:10.1097/HJH.0000000000001192.

3. **Chen CH, Nevo E, Fetics B, Pak PH, Yin FC, Maughan WL, Kass DA.** Estimation of central aortic pressure waveform by mathematical transformation of radial tonometry pressure. Validation of generalized transfer function. *Circulation* 95: 1827–1836, 1997. doi:10.1161/01.CIR.95.7.1827.
4. **Cho SK, Cho SK, Kim KH, Cho JY, Yoon HJ, Yoon NS, Hong YJ, Park HW, Kim JH, Ahn Y, Jeong MH, Cho JG, Park JC.** Effects of age on arterial stiffness and blood pressure variables in patients with newly diagnosed untreated hypertension. *Korean Circ J* 45: 44–50, 2015. doi:10.4070/kcj.2015.45.1.44.
5. **Cuomo F, Roccabianca S, Dillon-Murphy D, Xiao N, Humphrey JD, Figueroa CA.** Effects of age-associated regional changes in aortic stiffness on human hemodynamics revealed by computational modeling. *PLoS One* 12: e0173177, 2017. doi:10.1371/journal.pone.0173177.
6. **Cuomo F, Ferruzzi J, Agarwal P, Li C, Zhuang ZW, Humphrey JD, Figueroa CA.** Sex-dependent differences in central artery haemodynamics in normal and fibulin-5 deficient mice: implications for ageing. *Proc Math Phys Eng Sci* 475: 20180076, 2019. doi:10.1098/rspa.2018.0076.
7. **Dogui A, Kachenoura N, Frouin F, Lefort M, De Cesare A, Mousseaux E, Herment A.** Consistency of aortic distensibility and pulse wave velocity estimates with respect to the Bramwell-Hill theoretical model: a cardiovascular magnetic resonance study. *J Cardiovasc Magn Reson* 13: 11, 2011. doi:10.1186/1532-429X-13-11.
8. **Ebrahimi Nejad S, Carey JP, McMurtry MS, Hahn JO.** Model-based cardiovascular disease diagnosis: a preliminary in-silico study. *Biomech Model Mechanobiol* 16: 549–560, 2017. doi:10.1007/s10237-016-0836-8.
9. **Ganter MT, Alhashemi JA, Al-Shabasy AM, Schmid UM, Schott P, Shalabi SA, Badri AM, Hartnack S, Hofer CK.** Continuous cardiac output measurement by un-calibrated pulse wave analysis and pulmonary artery catheter in patients with septic shock. *J Clin Monit Comput* 30: 13–22, 2016. doi:10.1007/s10877-015-9672-0.
10. **Ghasemi Z, Lee JC, Kim CS, Cheng HM, Sung SH, Chen CH, Mukkamala R, Hahn JO.** Estimation of cardiovascular risk predictors from non-invasively measured diametric pulse volume waveforms via multiple measurement information fusion. *Sci Rep* 8: 10433, 2018. doi:10.1038/s41598-018-28604-6.
11. **Holenstein R, Niederer P, Anliker M.** A viscoelastic model for use in predicting arterial pulse waves. *J Biomech Eng* 102: 318–325, 1980. doi:10.1115/1.3138229.
12. **Jiang S, Zhang ZQ, Wang F, Wu JK.** A personalized-model-based central aortic pressure estimation method. *J Biomech* 49: 4098–4106, 2016. doi:10.1016/j.jbiomech.2016.11.007.
13. **Karamanoglu M, O'Rourke MF, Avolio AP, Kelly RP.** An analysis of the relationship between central aortic and peripheral upper limb pressure waves in man. *Eur Heart J* 14: 160–167, 1993. doi:10.1093/eurheartj/14.2.160.
14. **Kimoto E, Shoji T, Shinohara K, Inaba M, Okuno Y, Miki T, Koyama H, Emoto M, Nishizawa Y.** Preferential stiffening of central over peripheral arteries in type 2 diabetes. *Diabetes* 52: 448–452, 2003. doi:10.2337/diabetes.52.2.448.
15. **Langewouters GJ.** *Visco-elasticity of the Human Aorta in Vitro in Relation to Pressure and Age*. (PhD Thesis). Amsterdam: Free University of Amsterdam, 1982.
16. **Lee AJ, Cohn JH, Ranasinghe JS.** Cardiac output assessed by invasive and minimally invasive techniques. *Anesthesiol Res Pract* 2011: 475151, 2011. doi:10.1155/2011/475151.
17. **London GM, Blacher J, Pannier B, Guérin AP, Marchais SJ, Safar ME.** Arterial wave reflections and survival in end-stage renal failure. *Hypertension* 38: 434–438, 2001. doi:10.1161/01.HYP.38.3.434.
18. **Luzardo L, Lujambio I, Sottolano M, da Rosa A, Thijs L, Noboa O, Staessen JA, Boggia J.** 24-h ambulatory recording of aortic pulse wave velocity and central systolic augmentation: a feasibility study. *Hypertens Res* 35: 980–987, 2012. doi:10.1038/hr.2012.78.
19. **McEniery CM, Yasmin, Hall IR, Qasem A, Wilkinson IB, Cockcroft JR; ACCT Investigators.** Normal vascular aging: differential effects on wave reflection and aortic pulse wave velocity: the Anglo-Cardiff Collaborative Trial (ACCT). *J Am Coll Cardiol* 46: 1753–1760, 2005. doi:10.1016/j.jacc.2005.07.037.
20. **Mitchell GF, van Buchem MA, Sigurdsson S, Gotal JD, Jonsdottir MK, Kjartansson Ó, Garcia M, Aspelund T, Harris TB, Gudnason V, Launer LJ.** Arterial stiffness, pressure and flow pulsatility and brain structure and function: the Age, Gene/Environment Susceptibility – Reykjavik study. *Brain* 134: 3398–3407, 2011. doi:10.1093/brain/awr253.
21. **Mitchell GF, Hwang S-J, Vasan RS, Larson MG, Pencina MJ, Hamburg NM, Vita JA, Levy D, Benjamin EJ.** Arterial stiffness and cardiovascular events: the Framingham Heart Study. *Circulation* 121: 505–511, 2010. doi:10.1161/CIRCULATIONAHA.109.886655.
22. **Murgo JP, Westerhof N, Giolma JP, Altobelli SA.** Aortic input impedance in normal man: relationship to pressure wave forms. *Circulation* 62: 105–116, 1980. doi:10.1161/01.CIR.62.1.105.
23. **Natarajan K, Cheng HM, Liu J, Gao M, Sung SH, Chen CH, Hahn JO, Mukkamala R.** Central blood pressure monitoring via a standard automatic arm cuff. *Sci Rep* 7: 14441, 2017. doi:10.1038/s41598-017-14844-5.
24. **Nguyen LS, Squara P.** Non-invasive monitoring of cardiac output in critical care medicine. *Front Med (Lausanne)* 4: 200, 2017. doi:10.3389/fmed.2017.00200.
25. **O'Rourke MF, Pauca A, Jiang XJ.** Pulse wave analysis. *Br J Clin Pharmacol* 51: 507–522, 2001. doi:10.1046/j.0306-5251.2001.01400.x.
26. **Pagoulatou S, Stergiopulos N.** Evolution of aortic pressure during normal ageing: a model-based study. *PLoS One* 12: e0182173, 2017. doi:10.1371/journal.pone.0182173.
27. **Pagoulatou SZ, Stergiopulos N.** Estimating left ventricular elastance from aortic flow waveform, ventricular ejection fraction, and brachial pressure: an in silico study. *Ann Biomed Eng* 46: 1722–1735, 2018. doi:10.1007/s10439-018-2072-0.
28. **Papaioannou TG, Karageorgopoulou TD, Sergentanis TN, Protogerou AD, Psaltopoulou T, Sharman JE, Weber T, Blacher J, Daskalopoulou SS, Wassertheurer S, Khir AW, Vlachopoulos C, Stergiopulos N, Stefanadis C, Nichols WW, Tousoulis D.** Accuracy of commercial devices and methods for noninvasive estimation of aortic systolic blood pressure a systematic review and meta-analysis of invasive validation studies. *J Hypertens* 34: 1237–1248, 2016. doi:10.1097/HJH.0000000000000921.
29. **Papaioannou TG, Protogerou AD, Nasothimiou EG, Tzamouranis D, Skliros N, Achimastos A, Papadogiannis D, Stefanadis CI.** Assessment of differences between repeated pulse wave velocity measurements in terms of 'bias' in the extrapolated cardiovascular risk and the classification of aortic stiffness: is a single PWV measurement enough? *J Hum Hypertens* 26: 594–602, 2012. doi:10.1038/jhh.2011.76.
30. **Papaioannou TG, Protogerou AD, Stamatelopoulos KS, Vavuranakis M, Stefanadis C.** Non-invasive methods and techniques for central blood pressure estimation: procedures, validation, reproducibility and limitations. *Curr Pharm Des* 15: 245–253, 2009. doi:10.2174/138161209787354203.
31. **Papaioannou TG, Soulis D, Vardoulis O, Protogerou A, Sfikakis PP, Stergiopulos N, Stefanadis C.** First in vivo application and evaluation of a novel method for non-invasive estimation of cardiac output. *Med Eng Phys* 36: 1352–1357, 2014. doi:10.1016/j.medengphy.2014.06.019.
32. **Pauca AL, O'Rourke MF, Kon ND.** Prospective evaluation of a method for estimating ascending aortic pressure from the radial artery pressure waveform. *Hypertension* 38: 932–937, 2001. doi:10.1161/hy1001.096106.
33. **Protogerou AD, Argyris A, Nasothimiou E, Vrachatis D, Papaioannou TG, Tzamouranis D, Blacher J, Safar ME, Sfikakis P, Stergiou GS.** Feasibility and reproducibility of noninvasive 24-h ambulatory aortic blood pressure monitoring with a brachial cuff-based oscillometric device. *Am J Hypertens* 25: 876–882, 2012. doi:10.1038/ajh.2012.63.
34. **Quiñones MA, Otto CM, Stoddard M, Waggoner A, Zoghbi WA; Doppler Quantification Task Force of the Nomenclature and Standards Committee of the American Society of Echocardiography.** Recommendations for quantification of Doppler echocardiography: a report from the Doppler quantification task force of the nomenclature and standards committee of the American Society of Echocardiography. *J Am Soc Echocardiogr* 15: 167–184, 2002. doi:10.1067/mje.2002.120202.
35. **Redheuil A, Yu WC, Wu CO, Mousseaux E, de Cesare A, Yan R, Kachenoura N, Bluemke D, Lima JA.** Reduced ascending aortic strain and distensibility: earliest manifestations of vascular aging in humans. *Hypertension* 55: 319–326, 2010. doi:10.1161/HYPERTENSIONAHA.109.141275.
36. **Reference Values for Arterial Stiffness' Collaboration.** Determinants of pulse wave velocity in healthy people and in the presence of cardiovascular risk factors: 'establishing normal and reference values'. *Eur Heart J* 31: 2338–2350, 2010. doi:10.1093/eurheartj/ehq165.
37. **Reymond P, Bohraus Y, Perren F, Lazeyras F, Stergiopulos N.** Validation of a patient-specific one-dimensional model of the systemic arterial tree. *Am J Physiol Heart Circ Physiol* 301: H1173–H1182, 2011. doi:10.1152/ajpheart.00821.2010.

38. **Reymond P, Merenda F, Perren F, Rüfenacht D, Stergiopulos N.** Validation of a one-dimensional model of the systemic arterial tree. *Am J Physiol Heart Circ Physiol* 297: H208–H222, 2009. doi:10.1152/ajpheart.00037.2009.
39. **Reymond P, Westerhof N, Stergiopulos N.** Systolic hypertension mechanisms: effect of global and local proximal aorta stiffening on pulse pressure. *Ann Biomed Eng* 40: 742–749, 2012. doi:10.1007/s10439-011-0443-x.
40. **Sagawa K.** The end-systolic pressure-volume relation of the ventricle: definition, modifications and clinical use. *Circulation* 63: 1223–1227, 1981. doi:10.1161/01.CIR.63.6.1223.
41. **Stergiopulos N, Meister JJ, Westerhof N.** Evaluation of methods for estimation of total arterial compliance. *Am J Physiol* 268: H1540–H1548, 1995. doi:10.1152/ajpheart.1995.268.4.H1540.
42. **Suga H, Sagawa K.** Instantaneous pressure-volume relationships and their ratio in the excised, supported canine left ventricle. *Circ Res* 35: 117–126, 1974. doi:10.1161/01.RES.35.1.117.
43. **Tosello F, Guala A, Leone D, Camporeale C, Bruno G, Ridolfi L, Veglio F, Milan A.** Central pressure appraisal: clinical validation of a subject-specific mathematical model. *PLoS One* 11: e0151523, 2016. [Erratum in *PLoS One*, 11: e0157117, 2016.] doi:10.1371/journal.pone.0151523.
44. **Udy AA, Altukroni M, Jarrett P, Roberts JA, Lipman J.** A comparison of pulse contour wave analysis and ultrasonic cardiac output monitoring in the critically ill. *Anaesth Intensive Care* 40: 631–637, 2012. doi:10.1177/0310057X1204000408.
45. **Van Trijp MJ, Uiterwaal CS, Bos WJ, Oren A, Grobbee DE, Bots ML.** Noninvasive arterial measurements of vascular damage in healthy young adults: relation to coronary heart disease risk. *Ann Epidemiol* 16: 71–77, 2006. doi:10.1016/j.annepidem.2005.09.005.
46. **Vlachopoulos C, Aznaouridis K, O'Rourke MF, Safar ME, Baou K, Stefanadis C.** Prediction of cardiovascular events and all-cause mortality with central haemodynamics: a systematic review and meta-analysis. *Eur Heart J* 31: 1865–1871, 2010. doi:10.1093/eurheartj/ehq024.
47. **Wassertheurer S, Kropf J, Weber T, van der Giet M, Baulmann J, Ammer M, Hametner B, Mayer CC, Eber B, Magometschnigg D.** A new oscillometric method for pulse wave analysis: comparison with a common tonometric method. *J Hum Hypertens* 24: 498–504, 2010. doi:10.1038/jhh.2010.27.
48. **Weber T, Auer J, O'Rourke MF, Kvas E, Lassnig E, Lamm G, Stark N, Rammer M, Eber B.** Increased arterial wave reflections predict severe cardiovascular events in patients undergoing percutaneous coronary interventions. *Eur Heart J* 26: 2657–2663, 2005. doi:10.1093/eurheartj/ehi504.
49. **Weber T, Wassertheurer S, Rammer M, Maurer E, Hametner B, Mayer CC, Kropf J, Eber B.** Validation of a brachial cuff-based method for estimating central systolic blood pressure. *Hypertension* 58: 825–832, 2011. doi:10.1161/HYPERTENSIONAHA.111.176313.
50. **Wei W, Tölle M, Zidek W, van der Giet M.** Validation of the Mobil-O-Graph: 24 h-blood pressure measurement device. *Blood Press Monit* 15: 225–228, 2010. doi:10.1097/MBP.0b013e328338892f.
51. **Weiss W, Gohlisch C, Harsch-Gladisch C, Tölle M, Zidek W, van der Giet M.** Oscillometric estimation of central blood pressure: validation of the Mobil-O-Graph in comparison with the SphygmoCor device. *Blood Press Monit* 17: 128–131, 2012. doi:10.1097/MBP.0b013e328353ff63.
52. **Womersley J; Aeronautical Research Laboratory.** *An Elastic Tube Theory of Pulse Transmission and Oscillatory Flow in Mammalian Arteries*. Springfield, OH: Carpenter Lithographing & Printing, 1957.